Nanoembossing Induced Ferroelectric Lithography on PZT Films for Silver Particle Patterning

Zhenkui Shen,[†] Xinping Qu,[†] Yifang Chen,[‡,*] and Ran Liu[†,*]

[†]ASIC & System State Key Laboratory, Department of Microelectronics, Fudan University, Shanghai 200433, China and [‡]Rutherford Appleton Laboratory, Chilton, Didcot, Oxfordshire, OX11 0QX, United Kingdom

ABSTRACT The concept of growing nanosize particles on polarized ferroelectric domain areas is known as ferroelectric lithography (FL). Here, a further step of technical development was achieved by combining nanoembossing technique with the FL to realize the selective growth of silver on the polarized areas induced by nanoembossing. The induced rearrangements of domain distributions by embossing in the ferroelectric films have been characterized by piezoresponse force microscopy (PFM). The selective photochemical reduction of silver particles on the embossed nanostructures associated with the underlying domain patterns created by the nanoembossing process has been successfully demonstrated. This nanoembossing induced ferroelectric lithography (NIFL) developed in this work is expected to create an alternative route for nanoscale patterning of metals.

KEYWORDS: nanoembossing · ferroelectric PZT · domain · ferroelectric lithography · PFM

There have been considerable interests in developing new processes that can be used to synthesize nanostructures with complex functionality for various applications. Since Giocondi and Rohrer[1,2] reported the relationship between the surface photochemistry of $BaTiO_3$ and its underlying domain polarization in 2001, ferroelectric materials serving as photocatalysts in photochemistry have been widely studied. Kalinin *et al.*[3,4] proposed a novel method known as ferroelectric lithography, which has shown encouraging progress in recent years in the growth of 3D nanostructures on predefined locations of ferroelectric surfaces. This is attributed to the fact that a ferroelectric material with an internal dipolar field can effectively separate photogenerated electron–hole pairs *via* the bulk photovoltaic effect.[5] For instance, the dipole in domains with positive ferroelectric polarization is able to force the electrons in the conduction band to move toward its surface and thus induce local electrochemistry reactivity on the surface of the material.[6] Photochemical experiments on ferroelectrics[7,8] have shown that the reduction reactions (for example, the reduction of Ag^+ to Ag^0) are favored on the surface of positive domains. As the ferroelectric domain structures can be premodified, the surface of photochemical reaction can also be selected. Recently, this versatile method has found widespread applications in assembling and detecting nanostructural elements such as metal particles,[9–11] biological molecules,[12] and gases.[13] However, so far, the technique to perform ferroelectric lithography is mainly focused on ferroelectric domain writing using atomic force microscopy (AFM) with a conductive tip under an appropriate bias. Although it is a convenient method to pattern ferroelectric domains at the nanoscale, it is very limited in application due to both its slow scan rate and its small scan area. Therefore, better methods for ferroelectric lithography for future practical productions are urgently demanded. Nanoembossing is a rapid, specific, and cost-effective technology for large-scale polymer nanostructure fabrication in which surface patterns of a template are replicated into a material by mechanical contact and three-dimensional material displacements.[14,15] Lead zirconate titanate [$Pb(Zr_x,Ti_{1-x})O_3$] is one of the most intensively studied ferroelectrics and has been exploited as one of major materials in ferroelectric lithography due to its excellent property in large remnant polarization. In this work, nanoembossing induced ferroelectric lithography (NIFL) has been explored in nanoembossed $Pb(Zr_{0.3},Ti_{0.7})O_3$ (PZT) grating and dot nanostructure films. The induced rearrangements of domain patterns in the embossed films have been studied by piezoresponse force microscopy (PFM). It is found that photochemical growth of Ag particles is selectively distributed following the domain patterns generated by the nanoembossing process. Large arrays of silver patterns have been achieved. The results presented here indicate that it is

* Address correspondence to rliu@fudan.edu.cn, yifang.chen@stfc.ac.uk.

Received for review February 13, 2011 and accepted August 10, 2011.

Published online August 12, 2011
10.1021/nn202932z

feasible to directly perform nanoferroelectric lithography on nanoembossed ferroelectric films.

RESULTS AND DISCUSSION

The mechanism of domain selective photoreduction is briefly illustrated in Figure 1. Exposed to the super band gap UV light, electron−hole pairs can be generated and driven apart in the bulk of a ferroelectric material by the internal electric field. The mobile electrons could be forced to migrate to the surface of positive domains, and holes are driven away from it. If the material with positive domains is immersed into a metal salt solution, such as $AgNO_3$, the electrons can have reduction of Ag^+ to Ag on its surface, while with negative domains would not. In this way, photochemical patterning of metals on ferroelectric surfaces can be achieved.

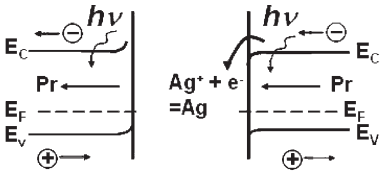

Figure 1. Band structures of a PZT film in contact with a $AgNO_3$ solution when irradiated to the UV light. The photogenerated electron−hole pairs are forced to the converse directions due to the different domain polarizations. The electrons driven to the surface can have reduction of Ag^+ to Ag.

Next, we investigated the feasibility to realize the photochemical FL using the nanoembossing technology. The process of nanoembossing on ferroelectric PZT films is schematically illustrated in Figure 2a. The spin-on films were first prebaked on a hot plate at 50 °C in air for 5 min to evaporate the solvent of the coated films and adjust the viscosity of the precursor. The

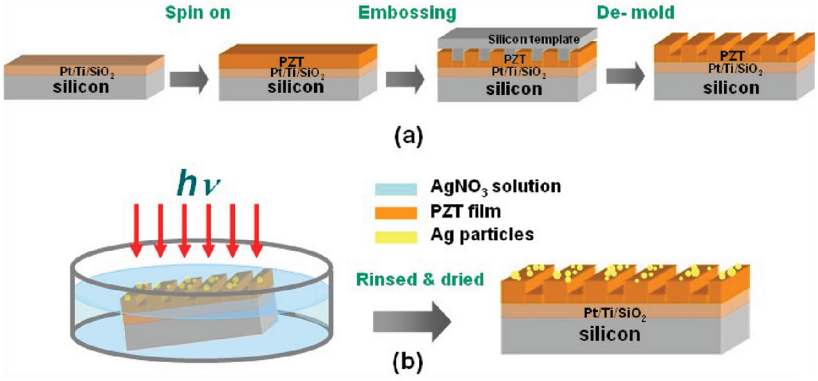

Figure 2. (a) Schematically illustration of ferroelectric PZT thin film nanoembossing process. (b) Sketch map of photochemical experiment on embossed PZT films.

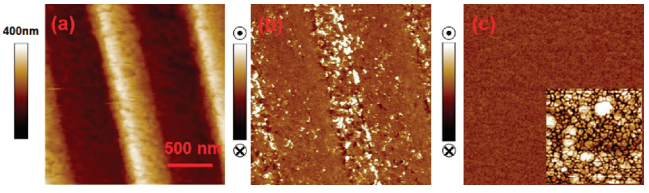

Figure 3. (a) Topography of an embossed PZT film with ~450 nm in total thickness. The embossed depth is ~200 nm. (b) Corresponding OPP image of the embossed region. The bright and dark contrasts represent domain with positive and negative polarization, respectively. (c) OPP signal from an unembossed region for comparison indicates a random domain state; inset is its related topography.

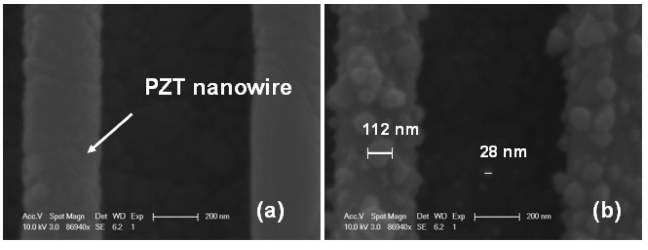

Figure 4. SEM pictures of embossed PZT topographies before (a) and after (b) Ag deposition, which clearly shows that Ag particles have selectively grown on the embossed nanowires attributed to the domain patterns created by the nanoembossing.

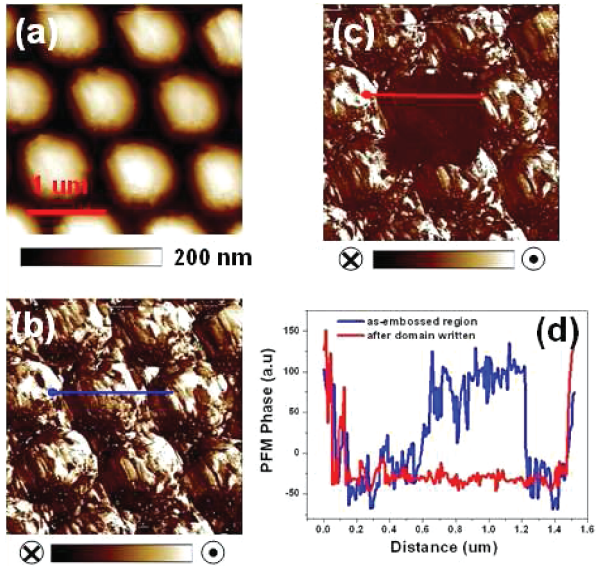

Figure 5. (a) Topography of the embossed dot structural PZT film with ~450 nm in total thickness. The embossed depth is ~150 nm. (b) Corresponding PFM phase image from the as-embossed region. (c) PFM phase image collected after applying 10 V within the center square which made a contrast change in this region. (d) Cross-sectional profiles from the blue line in (b) and red line in (c).

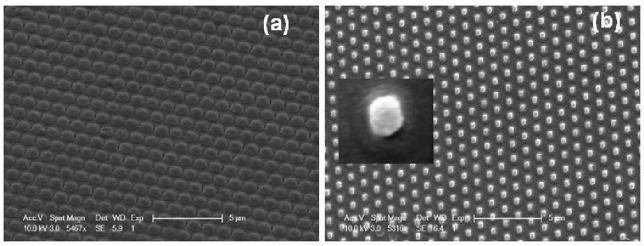

Figure 6. SEM pictures of the embossed PZT films before (a) and after (b) Ag deposition.

nanoembossing process was then carried out at room temperature under a pressure of 10−12 MPa for 15 min. After annealing, the embossed PZT films grown with the tetragonal structure and [111] preferred orientation were confirmed previously by both Raman spectroscopy (presented in Supporting Information Figure S1) and X-ray diffraction.[16] The embossed films exhibited good ferroelectric properties capable of demonstrating hysteresis loops (shown in Supporting Information Figure S2). Figure 3a presents the topography of the PZT film fabricated by a grating template. It can be seen that the grating structure is well transferred onto the film with ~200 nm embossed depth on a ~ 450 nm thick film. In order to map domain configurations, the PFM technique[17,18] has been applied on both embossed and unembossed regions for comparison. A PFM out-of-plane (OPP) phase image taken simultaneously from the embossed region is shown in Figure 3b. The bright area represents a domain polarization vector pointing upward (positive), whereas the dark area indicates the orientation of domain pointing downward (negative). Comparison between the embossed topography and the PFM data suggests that most domains with positive and negative polarizations incline to cluster along with the embossed nanowires. However, it is almost featureless with a random domain state for the unembossed region, as shown in Figure 3c (the corresponding topography is shown inset). There are several reports[19−22] suggesting that nanoembossing could be used to control the orientation of PVDF, one of the organic ferroelectrics. It seems to be well accepted that this is due to the thermomechanical history experienced by the polymer during the embossing process because the crystallization of the films is finished during the embossing process. There are also some reports on PZT nanoembossing,[23] in which the embossing process is completed at room temperature. That is to say, the stamping is done while the material is still in a gel form. However, the induced rearrangements of domain distributions in embossed films are still found. Unfortunately, these reports lack explanations on this phenomenon. We propose that this phenomenon might come from two ways: the pressure induced residue strain in the embossed gel films and the embossed nanostructures themselves. Both of them would have some influences on the domain

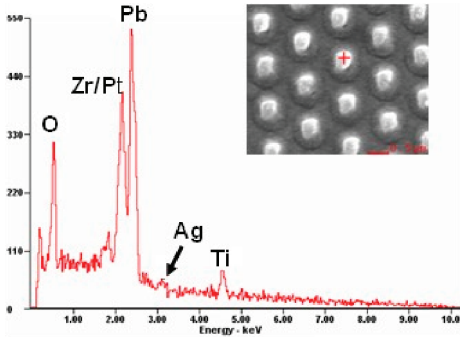

Figure 7. EDX measurement was performed, confirming the presence of silver particle deposition. Crossbar in the inset shows the spot of the spectra taken.

architectures during crystallization.[24,25] Dynamic crystallization of embossed PZT films still needs systemic work.

Photochemical experiments (Figure 2b) were sequentially carried out on the embossed grating film. By reducing a 0.01 M $AgNO_3$ solution under the UV irradiation for 15 min, Ag particles have been successfully deposited on the embossed grating structure PZT film, as seen in the SEM image (Figure 4b), in comparison with the as-embossed region (Figure 4a). Figure 4b shows that most of the Ag particles have selectively grown on the embossed nanowires with a much higher Ag particle density and larger size compared to the surface of the embossed bottom region. The average particles on the nanowires have reached the size of 90−120 nm in diameter, while few Ag particles of ∼20 nm in diameter, which are occasionally seen on the embossed bottom region, are still in the initial nucleation stage. This is due to the higher density positive domains created on the embossed nanowires, which drive more electrons to the surfaces of these regions and make them much richer in photogenerated electrons. Thus, the Ag particles that grow on these highly charged surfaces also present a higher growth rate than particles nucleating at lower charged interfaces.[26]

In order to demonstrate the flexibility of this technology, FL experiments on embossed PZT dot array films were further studied. Figure 5a shows the nanoembossed PZT dot array with ∼500 nm in diameter and ∼150 nm in embossed depth. Its corresponding PFM phase image is presented in Figure 5b, which indicates clustered positive domains distributed in the embossed central dot regions. To exclude possible topographic artifact in the domain structure measurements, ferroelectric domain switching experiment was performed. After 10 V bias was applied within the center square, the domain polarization in this region has been aligned to point downward, as can be seen in Figure 5c. The cross-sectional profiles (Figure 5d) from the PFM images confirm a change in sign of the phase of the PFM signal from the unwritten state (blue line) to the written state (red line), giving sufficient evidence that the contrasts in Figure 5b reflect the true domain state of the embossed film. Not surprisingly, by reducing a 0.1 M $AgNO_3$ solution under the UV irradiation for 20 min, silver particles have preferentially grown on the embossed PZT dot regions shown in Figure 6b. Compared to the as-embossed film (Figure 6a), it can be seen that highly ordered and large arrays of silver with ∼370 nm diameter have been patterned on the embossed PZT film. EDX measurement was executed to confirm the presence of silver particle deposition (Figure 7). The crossbar in the inset shows the spot of the spectra taken. Although the ferroelectric lithography with a probe tip using a bias is useful for fundamental studies, it is not feasible to apply it in practice.[3] Herein, nanoembossing induced ferroelectric lithography presents us a route to a large array of metal patterns by one-step exposure, which is more effective in practical applications. Nanoembossing has been applied to patterning structures in a number of materials with feature size down to ∼20 nm. However, the sol−gel-based PZT films generally consist of grains with size ranging from 60 to 100 nm, and works on PZT embossing reported so far have been limited to a minimum feature larger than 100 nm. It is, therefore, of great interest to further investigate nanoembossing of this material, study the related domain architectures, and possibly apply ferroelectric lithography at even smaller size.

CONCLUSION

In summary, a nanoembossing induced ferroelectric lithography (NIFL) by selective growth of metal particles on embossing induced polarized domains has been developed. Rearrangements of patterned domains in embossed films have been characterized by PFM measurements. We have demonstrated that, with the NIFL technique, it is possible to directly reduce metal salts on prepatterned ferroelectric nanostructures by nanoembossing without the

assistance of the external applied electric field. The technology developed here shows great advantages in rapid, low-cost, and large-scale processing and hence strong potential in future productions.

METHODS

PZT thin films were prepared on Pt/Ti/SiO_2/Si substrates by the sol–gel method with a ratio of 30:70. The raw materials were lead acetate trihydrate [$Pb(OCOCH_3)_2 \cdot 3H_2O$, 99.5%], zirconium tetra-*n*-propoxide ($Zr(OC_3H_8)_4$, 70%), and titanium(IV) butoxide ($Ti(OC_4H_9)_4$, 98%) as precursors and a methanol/acetic acid mixed solvent. Two different silicon templates were used for embossing, one is a grating with 500 nm wide lines and 1 μm wide pitch and the other is a dot array with 500 nm diameter and 1 μm pitch. Both templates were about 1 μm deep, prepared by e-beam lithography and dry etching. An antisticking layer was precoated on the silicon template surface in order to reduce their adhesion to PZT gels. After embossing, the gel layers were first pyrolyzed on a hot plate in air at 350 °C for 5 min. Crystallization was then initiated by a conventional thermal annealing process at 650 °C in air for 15 min.

PFM characterizations of domain configurations in the embossed film were carried out using an atomic force microscope (AFM) (Veeco Multimode V) in contact mode at room temperature. The piezoresponse signals collected using a lock-in amplifier and a Pt-coated AFM tip at a force constant of 0.03–0.2 N/m and a resonant frequency of 14–28 kHz. An ac voltage of 1 V at frequency of 100–200 kHz was applied to detect the piezoresponse signals from the samples. The average force on the cantilever was kept constant by a feedback loop during the scanning process. The electrical switching experiment on the embossed region was performed using the conducting tip biased at 10 V for negative domains writing.

Photochemical experiments were carried out by immersing the embossed PZT grating and dot structure films into fresh made $AgNO_3$ solutions with 0.01 and 0.1 M concentration, respectively. The pH value of the solutions was not adjusted and was used as it was. Then the samples were exposed to the UV radiation (Intelli-Ray 400 W Hg lamp). After exposure, the samples were rinsed by deionized water and blown dry with nitrogen gas. EDX spectra were acquired using a XL-30 FEG instrument.

Acknowledgment. This work was financially supported by National Basic Research Program of China (2011CBA00603) and the 985" Micro/nanoelectronics Science and Technology Innovation Platform at Fudan University.

Supporting Information Available: Additional supporting figures. This material is available free of charge *via* the Internet at http://pubs.acs.org.

REFERENCES AND NOTES

1. Giocondi, J. L.; Rohrer, G. S. Spatially Selective Photochemical Reduction of Silver on the Surface of Ferroelectric Barium Titanate. *Chem. Mater.* **2001**, *13*, 241–242.
2. Giocondi, J. L.; Rohrer, G. S. Spatial Separation of Photochemical Oxidation and Reduction Reactions on the Surface of Ferroelectric $BaTiO_3$. *J. Phys. Chem. B* **2001**, *105*, 8275–8277.
3. Kalinin, S. V.; Bonnell, D. A.; Alvarez, T.; Lei, X.; Hu, Z.; Ferris, J. H.; Zhang, Q.; Dunn, S. Atomic Polarization and Local Reactivity on Ferroelectric Surfaces: A New Route toward Complex Nanostructures. *Nano Lett.* **2002**, *2*, 589–593.
4. Kalinin, S. V.; Bonnell, D. A.; Alvarez, T.; Lei, X.; Hu, Z.; Shao, R.; Ferris, J. H. Ferroelectric Lithography of Multicomponent Nanostructrues. *Adv. Mater.* **2004**, *16*, 795–799.
5. Tiwari, D.; Dunn, S. Photochemistry on a Polarisable Semiconductor: What Do We Understand Today? *J. Mater. Sci.* **2009**, *44*, 5063–5079.
6. Rankin, C.; Chou, C. H.; Conklin, D.; Bonnell, D. A. Polarization and Local Reactivity on Organic Ferroelectric Surfaces: Ferroelectric Nanolithography Using Poly(vinylidene fluoride). *ACS Nano* **2007**, *1*, 234–238.
7. Bhardwaj, A.; Burbure, N. V.; Gamalski, A.; Rohrer, G. S. Composition Dependence of the Photochemical Reduction of Ag by $Ba_{1-x}Sr_xTiO_3$. *Chem. Mater.* **2010**, *22*, 3527–3543.
8. Burbure, N. V.; Salvador, P. A.; Rohrer, G. S. Photochemical Reativeity of Titania Films on $BaTiO_3$ Substrates: Influence of Titania Phase and Orientation. *Chem. Mater.* **2010**, *22*, 5831–5837.
9. Dunn, S.; Jones, P. M.; Gallardo, D. E. Photochemical Growth of Silver Nanoparticles on c^- and c^+ Domain on Lead Zirconate Titanate Thin Films. *J. Am. Chem. Soc.* **2007**, *129*, 8724–8728.
10. Jones, P. M.; Dunn, S. Photo-reduction of Silver Salts on Highly Hereogeneous Lead Zirconate Titanate. *Nanotechnology* **2007**, *18*, 185702–185707.
11. Jones, P. M.; Dunn, S. Interaction of Stern Layer and Domain Structure on Photochemistry of Lead-Zirconate-Titanate. *Nanotechnology* **2009**, *42*, 065408–065412.
12. Dunn, S.; Cullen, D.; Abad-Garcia, E.; Bertoni, C.; Carter, R. Using the Surface Spontaneous Depolarization Field of Ferroelectrics To Direct the Assembly of Virus Particles. *Appl. Phys. Lett.* **2004**, *85*, 3537–3539.
13. Li, D.; Zhao, M. H.; Garra, J.; Kolpak, A. M.; Rappe, A. M.; Bonnell, D. A.; Vohs, J. M. Direct *In Situ* Determination of the Polarization Dependence of Physisorption on Ferroelectric Surfaces. *Nat. Mater.* **2008**, *7*, 473–477.
14. Schift, H. Nanoimprint Lithography: An Old Story in Modern Times? A Review. *J. Vac. Sci. Technol., B* **2008**, *26*, 458–480.
15. Guo, L. J. Nanoimprint Lithography: Methods and Material Requirements. *Adv. Mater.* **2007**, *19*, 495–513.
16. Shen, Z. K.; Chen, Z. H.; Qiu, Z. J.; Lu, B. R.; Wan, J.; Deng, S. R.; Jiang, A. Q.; Qu, X. P.; Liu, R.; Chen, Y. F. Influences of Embossing Technology on Ferroelectric Thin Film. *Microelectron. Eng.* **2010**, *87*, 869–871.
17. Gruverman, A.; Kalinin, S. V. Piezoresponse Force Microscopy and Recent Advances in Nanoscale Studies of Ferroelectrics. *J. Mater. Sci.* **2006**, *41*, 107–116.
18. Gruverman, A.; Kholkin, A. Nanoscale Ferroelectrics: Processing, Characterization and Future Trend. *Rep. Prog. Phys.* **2006**, *69*, 2443–2474.
19. Hu, Z.; Tian, M.; Nysten, B.; Jonas, A. M. Regular Arrays of Highly Ordered Ferroelectric Polymer Nanostructures for Non-volatile Low-Voltage Memories. *Nat. Mater.* **2009**, *8*, 62–67.
20. Liu, Y.; Weiss, D. N.; Li, J. Rapid Nanoimprint and Excellent Piezoresponse of Polymeric Ferroelectric Nanostructures. *ACS Nano* **2010**, *4*, 83–90.
21. Hu, Z.; Baralia, G.; Bayot, V.; Gohy, J. F.; Jonas, A. M. Nanoscale Control of Polymer Crystallization by Nanoimprint Lithography. *Nano Lett.* **2005**, *5*, 1738–1743.
22. Brian, C. O.; Christopher, L. S.; Jack, F. D.; Hyun, W. R.; Alamgir, K.; Daniel, R. H. Crystallization of Poly(ethylene oxide) Patterned by Nanoimprint Lithgraphy. *Macromolecules* **2007**, *40*, 2968–2970.
23. Lan, L.; Xie, S.; Tan, L.; Li, J. Sol–Gel Based Soft Lithography and Piezoresponse Force Microscopy of Patterned Pb-$(Zr_{0.52}Ti_{0.48})O_3$ Microstructures. *J. Mater. Sci. Technol.* **2010**, *26*, 439–444.
24. Rodriguez, B. J.; Gao, X. S.; Liu, L. F.; Lee, W.; Naumov, I. I.; Bratkovsky, A. M.; Hesse, D.; Alexe, M. Vortex Polarization States in Nanoscale Ferroelectric Arrays. *Nano Lett.* **2009**, *9*, 1127–1131.

25. Schilling, A.; Bowman, R. M.; Catalan, G.; Scott, J. F.; Gregg, J. M. Morphological Control of Polar Orientation in Single-Crystal Ferroelectric Nanowires. *Nano Lett.* **2007**, *7*, 3787–3791.
26. Dunn, S.; Sharp, S.; Burgess, S. The Photochemical Growth of Silver Nanoparticle on Semiconductor-Initial Nucleation Stage. *Nanotechnology* **2009**, *20*, 115604–115609.